PAPER • **OPEN ACCESS**

A Response Surface Methodology for Mitigating Hot Gasses in Enclosed Car Park

A Response Surface Methodology for Mitigating Hot Gasses in Enclosed Car Park

Ahmad Faiz Tharima, **Mohd Zamri Yusoff, Md Mujibur Rahman**

College of Engineering, Universiti Tenaga Nasional (UNITEN), Putrajaya Campus, Jalan IKRAM-UNITEN, 43000 Kajang, Selangor, Malaysia.

Email: pait.afz@gmail.com

Abstract A hot gas rise towards ceiling due to fire buoyancy will cause severe damage to the building structure. The temperature rises need to be controlled as among the elements of compliance in performance-based design. The channel flow between beams has used in this study to mitigate hot gases out of the enclosure by mean of response surface methodology. Fire Dynamic Simulator was employed as a simulation tool while the result was statistically examined using analysis of variance via Minitab application. It was found that the result was linear with predicted R^2 (93.25%) and within the permissible R^2 (98.13%). The ceiling height has been identified not affect in controlling hot gases while four control parameters which are beam spacing, transversal beam, extraction rate and longitudinal beam with p-values of 0.00, 0.000, 0.023 and 0.000 respectively, have been found to have the significant effect on the smoke temperature control. This study contributes a good input to the fire safety community in providing the initial design of enclosed car park with better condition.

1 Introduction

The temperatures rise need to be controlled as among the elements of compliance in performance-based design as well as in perceptive code. A hot gas rise towards ceiling due to fire buoyancy will reduce oxygen concentration eventually create harmful to an occupants [1] and cause severe damage to the building structure such as enclosed car park [2], subway station [3] corridor -like structures [4], tunnel-like corridor [5] and underground shelter [6] as well as others building.

The fire temperatures measurement is essential to predict ignition of the object, the onset of flashover and structure damage [7]. Apart of that, it is also beneficial for predict smoke layer descent towards the floor [8] and arranges for a smoke detection [9–11] as well as sprinkler activation [12]. Following that, previous researchers had developed various ratio from experimental and numerical simulation such as beam depth to the ceiling height [13–15], radial distance to the ceiling height [16], beam spacing to ceiling clearance [15]. Most of it is to investigate the effect of the ceiling beam against flow visualization, temperature and velocity profile. In addition, it also can identify subcritical flow or density jump before and after ceiling jet intersect the ceiling beam.

However, according to the literature [11–15], most studies were conducted by means of trial and error based. These arrangements have not yet statistically proofed and which parameters show the significant effect of the temperature. In addition, the parameters that were investigated such as heat release rate (HRR) and the wind were categorized as non-control factors. Indeed, a few research papers related to the hot smoke control with the presence of the beam has been reported by [13–15,19,22–27] but still lacking regarding cost operational reducing (i.e in term of horizontal ventilation numbers and volume flow rate). Therefore, this study aims to channel the hot gasses by means statistical analysis based on established control parameters and resulting in the optimum operational cost of the ventilation fan.

2 Method

The research procedures were designed in the following steps [29]:
(a) identify the significant controllable factors
(b) performing the Design of Experiment (DOE)
(c) performing Computational Fluid Dynamics (CFD) simulation
(d) conducting the reliability test of DOE
(e) performing statistical analysis

2.1 Controllable Factors

The key factors that influence the temperature was identified which are ceiling height, beam span length, transversal beam depth, longitudinal beam depth and extraction fan rate [13–16]. The range of these factors is reported in Table 1. According to a general rule of Reynolds number, the ceiling height range from the literature review was changed to 0.3m due to the smallest height that supports turbulent flow is 0.3m [30,31]. The other amendment made within this range is beam span length; 0.556m to 0.57m in accordance to actual geometry size in Simulator Building at Fire and Rescue Malaysia Academy.

Table 1. Factor and response parameters

Parameters	Name	Coded Factor	Lower	Upper
Factors	Ceiling Height,	X	0.3m	0.442m
	Beam Span Length,	X_1	0.213m	0.57m
	Transversal Beam Depth,	X_2	0.02m	0.06m
	Extraction Fan Rate	X_3	$0.18m^3/s$	$0.31m^3/s$
	Longitudinal Beam Depth	X_4	0.02m	0.061m
Response	Temperature	Y		

2.2 Design of Experiment

The selected DOE was Central Composite Design (CCD) because it incorporates better design points. Correspondingly, the Face Central Design was employed to obtain the 32 design points. In order to maintain a hierarchical model at each step, terms were added during the process by using the stepwise procedure. The design points and their corresponding results are reported in Table 2.

Table 2. Numerical simulation design and results

Run	Factors					Temperature
	X	X_1	X_2	X_3	X_4	Y
1	0.442	0.213	0.02	0.31	0.061	315.97
2	0.371	0.3915	0.04	0.245	0.02	185.51
3	0.3	0.57	0.06	0.18	0.061	163.45
4	0.3	0.57	0.06	0.31	0.02	115.67
5	0.3	0.213	0.02	0.31	0.02	253.63
6	0.371	0.3915	0.04	0.245	0.0405	215.69
7	0.371	0.3915	0.04	0.245	0.0405	203.70
8	0.3	0.57	0.02	0.18	0.02	181.76
9	0.442	0.213	0.06	0.18	0.061	216.17
10	0.371	0.3915	0.04	0.18	0.0405	212.89
11	0.371	0.213	0.04	0.245	0.0405	231.64
12	0.371	0.3915	0.04	0.245	0.061	225.11
13	0.442	0.57	0.06	0.18	0.02	162.44
14	0.3	0.3915	0.04	0.245	0.0405	215.46
15	0.371	0.3915	0.04	0.245	0.0405	215.61
16	0.371	0.3915	0.04	0.31	0.0405	201.17
17	0.442	0.213	0.02	0.18	0.02	223.52
18	0.371	0.57	0.04	0.245	0.0405	179.82
19	0.371	0.3915	0.02	0.245	0.0405	262.6
20	0.3	0.213	0.06	0.31	0.061	265.12
21	0.3	0.213	0.02	0.18	0.061	398.07
22	0.371	0.3915	0.04	0.245	0.0405	197.79
23	0.371	0.3915	0.04	0.245	0.0405	211.11
24	0.442	0.213	0.06	0.31	0.02	181.86
25	0.442	0.57	0.06	0.31	0.061	185.51
26	0.3	0.213	0.06	0.18	0.02	125.71
27	0.442	0.57	0.02	0.31	0.02	206.29
28	0.371	0.3915	0.04	0.245	0.0405	205.38
29	0.442	0.57	0.02	0.18	0.061	223.92
30	0.371	0.3915	0.06	0.245	0.0405	193.45
31	0.3	0.57	0.02	0.31	0.061	278.27
32	0.442	0.3915	0.04	0.245	0.0405	209.38

2.3 CFD Simulation

The computational fluid dynamics (CFD) simulation was performed by using FDS software, which is specialized software in modelling fire-driven fluid flow. Flow turbulence was modelled via Large Eddy Simulation. Table 3 shows the numerical settings of the simulation.

Table 3. Numerical setting for the simulation

Parameter	Description of Car Park
Geometry dimension	4m x 1.6m x 0.3m
Mesh size	0.0094m
HRRPUA	2842.7kW/m^2
Fuel	Propane (C_3H_8)
CO yield	0.005
Soot yield	0.024
Fire source area	0.11684m x 0.0762m

2.3.1 Boundary conditions

- The ceiling, floor and side walls were prescribed as inert boundaries.
- The surrounding environment was not modelled. The ambient temperature was simply prescribed as 30ºC.
- The wind effects were not considered.
- Two longitudinal beams placed at the center of car park were supported by transversal beams and columns of different sizes.
- The smoke extraction rate was specified at the downstream opening which was positioned below the transversal beam depth.
- The size of fuel source area was 0.11684m x 0.0762m with height of 0.02667 m.

2.3.2 Conservation Equation

The mass (1) momentum (2) and energy (3) conservation equations can be written as:

$$\frac{\partial \rho}{\partial t} + \nabla . \rho \mathrm{u} = \dot{\mathrm{m}}_{\mathrm{b}}''' \quad (1)$$

$$\frac{\partial}{\partial t}(\rho \mathrm{u}) + \nabla \cdot \rho \mathrm{uu} + \nabla p = \rho g + \mathrm{f_b} + \nabla \cdot \tau_{\mathrm{ij}} \quad (2)$$

$$\frac{\partial}{\partial t}(\rho \mathrm{h}) + \nabla \cdot \rho \mathrm{hu} = \frac{\mathrm{Dp}}{\mathrm{Dt}} + \dot{\mathrm{q}}''' - \dot{\mathrm{q}}_{\mathrm{b}}''' - \nabla \cdot \mathrm{q}''' \quad (3)$$

In these equations, ρ is density, t is time, $\mathbf{u}$ is velocity vector, $\dot{\mathrm{m}}_{\mathrm{b}}'''$ is net heat flux from thermal conduction and radiation, p is pressure, $\boldsymbol{g}$ is gravity vector, $\mathbf{f}_{\mathrm{b}}$ is external force vector, τ_{ij} is viscous stress tensor, $\dot{\mathrm{q}}'''$ is heat release rate per unit volume from a chemical reaction, $\dot{\mathrm{q}}_{\mathrm{b}}'''$ is energy transferred to the evaporating droplets, $\dot{\mathbf{q}}''$ is conductive and radiative heat flux and ε is dissipation rate.

2.4 Reliability of DOE

The reliability of the DOE model was performed using the replication procedure which requires six models. As shown in Table 4, the results are ranging from 0.52% to 4.44%, indicating that the model is reliable.

Table 4. Replication of an enclosed car park model

Factors					Response	Error
Ceiling Height	Beam Span Length	Transversal Beam Depth	Extraction Rate	Longitudinal Beam Depth	Temperature	
0.371	0.3915	0.04	0.245	0.0405	205.11	0.65
0.371	0.3915	0.04	0.245	0.0405	203.7	1.33
0.371	0.3915	0.04	0.245	0.0405	215.61	4.44
0.371	0.3915	0.04	0.245	0.0405	197.79	4.19
0.371	0.3915	0.04	0.245	0.0405	211.11	2.26
0.371	0.3915	0.04	0.245	0.0405	205.38	0.52

2.5 Statistical Analysis

The form of mathematical model is as follows:

$$y = \propto_0 + \sum_{i=1}^{3} \propto_i x_i + \sum_{i=1}^{3} \propto_{ii} x_i^2 + \sum_{i=1}^{2} \sum_{j=i+1}^{3} \propto_{ij} x_i x_j \quad (4)$$

Where y is the predicted response (hot gases temperature); x_i and x_j are the uncoded independent variables and $\propto_0, \propto_i, \propto_{ii}$ *and* $\propto_{ij}$ are intercept, linear, quadratic and interaction constant coefficient respectively. Minitab was used for regression analysis and analysis of variance (ANOVA).

3 Results

3.1 Mesh independence Test and Geometry Validation

This model has been verified using a grid independence test and validated using a relative error percentage [32]. The grid independence study showed the finer mesh count was sufficient to conduct a further simulation. Moreover, the finest mesh was resulting in the lowest error with only 4.33%. The readers are referred to [33] for a complete description of the numerical experiment. Besides, a geometric validation also was performed between an enclosed car park and corridor-like structures experimented by Ji et al., (2015). According to Figure 1, it shows a similar pattern and indicating the enclosed car park design is good agreement with corridor-like structures simulation.

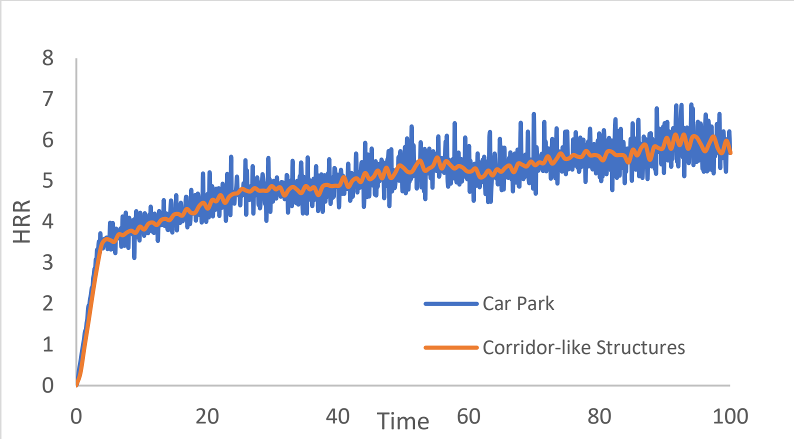

Figure 1. HRR for corridor-like structures fire and car park

3.2 Regression model

The relationship between temperature and five controllable factors (namely ceiling height X, beam span length X_1, transversal beam depth X_2, longitudinal beam depth X_3 and extraction rate X_4) was studied. The simulation result based on CCD model has developed a full quadratic equation as follows: -

$$y = 360.9 - 265X - 365.0X_1 - 8401X_2 + 81.7X_3 + 8032X_4 + 31285X_2^2 + 710XX_1 + 9598XX_2 - 11194XX_4 + 2436X_1X_2 - 3584X_1X_4 - 16229X_2X_4 \quad (5)$$

Based on statistical analysis, the result was linear with predicted R^2 (93.25%) and within the permissible R^2 (98.13%). It was found that the result was linear and good agreement can be seen between actual and predicted values.

3.3 ANOVA

Table 5 shows the linear, interaction and quadratic variables for the coded coefficient. In ANOVA analysis, the terms that found statistically significant only will be included in the model. Each variable with P-value less than 0.01 is considered highly significant, and between 0.01 and 0.05 is significant. The variable with P-value more than 0.05 is considered non-significant [34]. In the present work, it is observed that most of the variables have a highly significant on the linear effect, interaction and second order form. Only the ceiling height term in the linear effect was not significant. This illustrates the importance of employing the significant variables in design lower temperature in the enclosed car park.

Table 5. Coded Coefficients for Transformed Response

Coded Factor	Effect	Coef	SE Coef	T-Value	P-Value	Degree of Importance
X	-8.01	-4.00	2.15	-1.87	0.078	Non- significant
X_1	-57.17	-28.59	2.15	-13.32	0.000	High significant
X_2	-81.63	-40.81	2.15	-19.01	0.000	High significant
X_3	10.62	5.31	2.15	2.47	0.023	significant
X_4	70.58	35.29	2.15	16.44	0.000	High significant
X_2^2	25.03	12.51	3.25	3.86	0.001	Significant
XX_1	18.00	9.00	2.28	3.95	0.001	High significant
XX_2	27.26	13.63	2.28	5.99	0.000	High significant
XX_4	-32.58	-16.29	2.28	-7.16	0.000	High significant
X_1X_2	17.40	8.70	2.28	3.82	0.001	High significant
X_1X_4	-28.20	-14.10	2.28	-6.19	0.000	High significant
X_2X_4	-13.31	-6.65	2.28	- 2.92	0.009	High significant

Finally, based on P-value discussed above and significant effect, only the ceiling height term in the linear effect was not significant and should be removed. Thus, the model can be summarized as the following equation:

$$y = 360.9 - 365.0X_1 - 8401X_2 + 81.7X_3 + 8032X_4 + 31285X_2^2 + 710XX_1 + 9598XX_2 - 11194XX_4 + 2436X_1X_2 - 3584X_1X_4 - 16229X_2X_4 \quad (6)$$

4 Conclusion

In this research, the influence hot gasses temperature is investigated with identified factors such as ceiling height, beam span length, transversal and longitudinal beam depth, as well as extraction rate. For that purposes, the Response Surface Methodology (RSM) and Fire Dynamic Simulator (FDS) were used as a tool. The reliability result showed RSM can be used to investigate the controllable probability factors that influenced the response. In accordance to that, four factors have confirmed effect temperature in an enclosed car park. With only important parameters were included in this study, it is considered novelty in yielding lower temperature for the overall of car park geometry. The engineers afterwards could only have considered the high significant factors mentioned above in their design as compared to others factors studied in the previous study.

Acknowledgements:
This study work is supported by the scholarship provided by Malaysia Public Service Department to the first author.

References

[1] X.G. Zhang, Y.C. Guo, C.K. Chan, W.Y. Lin, Numerical simulations on fire spread and smoke movement in an underground car park, Build. Environ. 42 (2007) 3466–3475. doi:10.1016/j.buildenv.2006.11.002.
[2] M. Zahirasri, Multiple Vehicle Design Fire Scenarios in Car Parking Buildings by, (2015).
[3] N. Meng, L. Hu, S. Zhu, L. Yang, Effect of smoke screen height on smoke flow temperature profile beneath platform ceiling of subway station: An experimental investigation and scaling correlation, Tunn. Undergr. Sp. Technol. 43 (2014) 204–212. doi:10.1016/j.tust.2014.05.008.
[4] J. Ji, Y.Y. Fu, C.G. Fan, Z.H. Gao, K.Y. Li, An experimental investigation on thermal characteristics of sidewall fires in corridor-like structures with varying width, Int. J. Heat Mass Transf. 84 (2015) 562–570. doi:10.1016/j.ijheatmasstransfer.2015.01.020.
[5] T. Beji, S. Ukleja, J. Zhang., M.A. Delichatsios, Fire behaviour and external flames in corridor and tunnel-like enclosures, FIRE Mater. (2012). doi:10.1002/fam.
[6] A. Mukhtar, N.K. Ching, M.Z. Yusoff, Optimal Design of Opening Ventilation Shaft by

Kriging Metamodel Assisted Multi-objective Genetic Algorithm, 7 (2017). doi:10.7763/IJMO.2017.V7.565.
[7] W.D.W. and P.H. Thomas, Estimating Temperatures in Compartment Fires, in: SFPE Handb. Fire Prot. Eng., 2nd ed., 1995.
[8] E.K. Budnick, D.D. Evans, H.E. Nelson, Simplified Fire Growth Calculations, in: Fire Prot. Handb., 19th ed., 2003.
[9] M. He, Y. Jiang, J. Vythoulkas, T. AI-Farra, Smoke Detector Performance For Level Ceiling With Deep Beams and Deep Beam Pocket Configuration, Igarss 2014. (2014) 1–5. doi:10.1007/s13398-014-0173-7.2.
[10] F. J, R. S, G. D, Evaluating Smoke Detector Spacing Requirements for Parallel Beamed Hallways and Sloped Ceilings, Igarss 2014. (2014) 1–5. doi:10.1007/s13398-014-0173-7.2.
[11] F. G.P, D. W.D, K. J.H, Simulating the Effect of Beamed Ceilings on Smoke Flow , Part I . Comparison of Numerical and Experimental Results, (1992).
[12] R. Vettori, Effect of a Beamed, Sloped, and Sloped Beamed Ceilings on the Activation Time of a Residential Sprinkler, (2003).
[13] C.C. Koslowski, V. Motevalli, Effect of Beams on Ceiling Jet Behavior and Heat Detector Operation, J. Fire Prot. Eng. 5 (1993) 97–111. doi:10.1177/104239159300500302.
[14] C. Koslowski, V. Motevalli, Behavior of a 2-Dimensional Ceiling Jet Flow : A Beamed Ceiling Configuration, (1994) 469–480.
[15] Delichatsios, The Flow of Fire Gases Under a Beamed Ceiling, 10 (1981).
[16] N. Johansson, J. Wahlqvist, P. Van Hees, Numerical experiments in fire science : a study of ceiling jets, (2014). doi:10.1002/fam.
[17] N. Johansson, Numerical experiments and compartment fires, Fire Sci. Rev. 3 (2014) 2. doi:10.1186/s40038-014-0002-2.
[18] X. Deckers, S. Haga, N. Tilley, B. Merci, Smoke control in case of fire in a large car park: CFD simulations of full-scale configurations, Fire Saf. J. 57 (2013) 22–34. doi:10.1016/j.firesaf.2012.02.005.
[19] X. Deckers, S. Haga, B. Sette, B. Merci, Smoke control in case of fire in a large car park : Full-scale experiments, Fire Saf. J. 57 (2013) 11–21. doi:10.1016/j.firesaf.2012.10.017.
[20] C.-H. Hwang, a. Lock, M. Bundy, E. Johnsson, Studies on Fire Characteristics in Over- and Underventilated Full-scale Compartments, J. Fire Sci. 28 (2010) 459–486. doi:10.1177/0734904110363106.
[21] L.H. Hu, L.F. Chen, W. Tang, A global model on temperature profile of buoyant ceiling gas flow in a channel with combining mass and heat loss due to ceiling extraction and longitudinal forced air flow, Int. J. Heat Mass Transf. 79 (2014) 885–892. doi:10.1016/j.ijheatmasstransfer.2014.08.045.
[22] Deckers, Haga, Tilley, Merci, Smoke control in case of fire in a large car park: CFD simulations of full-scale configurations, Fire Saf. J. 57 (2013) 22–34. doi:10.1016/j.firesaf.2012.02.005.
[23] M. Deckers, Haga, Tilley, Smoke control in case of fire in a large car park: Full-scale experiments, Fire Saf. J. 57 (2013) 22–34. doi:10.1016/j.firesaf.2012.02.005.
[24] V. Motevalli, Z.P. Yuan, Steady State Ceiling Jet Behavior under an Unconfined Ceiling with Beams, Fire Technol. 44 (2008) 97–112. doi:10.1007/s10694-007-0027-3.
[25] Hinkley, Smoke & Heat Venting, in: SFPE Handb. Fire Prot. Eng., 2nd ed., 1995.
[26] J.H. Klote, J.A. Milke, Principles of smoke management, in: Princ. Smoke Manag., 2002.
[27] J.H. Klote, The ASHRAE design manual for smoke control, Fire Saf. J. 7 (1984) 93–98. doi:10.1016/0379-7112(84)90012-2.
[28] F.D. Simulations, Guide Guide for the Verification and Validation of Computational Fluid Dynamics Simulations, 1998 (2002).
[29] V. Gunaraj, N. Murugan, Application of response surface methodology for predicting weld bead quality in submerged arc welding of pipes, J. Mater. Process. Technol. 88 (1999) 266–

275. doi:10.1016/S0924-0136(98)00405-1.
[30] J.G. Quintiere, M.E. Dillon, Scale Model Reconstruction of Fire in an Atrium, Prog. Scale Model. (2008) 109–120.
[31] J.H. Klote, Scaling Modeling, in: Handb. Smoke Control Eng., 2012: p. xxiii, 484 .
[32] A.P. Smardz, Validation of Fire Dynamics Simulator (FDS) for forced and natural convection flows, 2006 (2006).
[33] A. Faiz Tharima, M. Mujibur Rahman, M. Zamri Yusoff, Verification and Validation of Fire Dynamic Simulator for Enclosed Car Park, Int. J. Model. Optim. 7 (2017) 105–108. doi:10.7763/IJMO.2017.V7.567.
[34] A.M. Doust, M. Rahimi, M. Feyzi, An Optimization Study by Response Surface Methodology (RSM) on Viscosity Reduction of Residue Fuel Oil Exposed Ultrasonic Waves and Solvent Injection, Iran. J. Chem. Eng. 13 (2016) 3–19.